J. CHEM. SOC. FARADAY TRANS., 1994, 90(23), 3491-3503

Molecular Structures of *cis*- and *trans*-*S*-Ethyl Thiocrotonate

A Combined Vibrational Spectroscopic and *Ab Initio* SCF-MO Study

Rui Fausto*
Departamento de Química, Universidade de Coimbra, P-3049 Coimbra, Portugal
Peter J. Tonge
The Picower Institute for Medical Research, Manhasset, NY 11030, USA
Paul R. Carey
Department of Biochemistry, University of Ottawa, Ottawa, Ontario, Canada K1H 8M5

Ab initio 6-31G* SCF-MO calculations have been carried out for *cis*- and *trans*-*S*-ethyl thiocrotonate [*cis*- and *trans*- $CH_3-CH=CH-C(=O)SCH_2CH_3$]. Fully optimized geometries, relative stabilities, dipole moments and harmonic force fields for several conformers of these molecules have been determined and the results compared with those of similar molecules. Combined with FTIR spectroscopic data, the theoretical results demonstrate that *trans*-*S*-ethyl thiocrotonate exists in two different conformations about the $C_\alpha-C$ bond (the *s*-*cis* and *s*-*trans* forms, with C=C—C=O dihedral angles equal to 0° and 180°, respectively), the *s*-*cis* conformation being more stable than the *s*-*trans* form by *ca.* 7 kJ mol^{-1} for the isolated molecule situation, while the *cis*-*s*-ethyl thiocrotonate molecule adopts only the *s*-*cis* conformation about this bond. A comparison of the experimental and theoretical vibrational spectra also shows that the existence of the less stable *s*-*trans* isomer of an α,β-unsaturated thioester can be successfully monitored by the IR band at *ca.* 1165 cm^{-1}, ascribed to the $C_\alpha-C$ stretching mode of this form. Additional conformationally sensitive bands are also identified, but these are difficult to use in the IR spectrum because of overlap with other features.

Resonance Raman spectroscopic studies of enzyme–substrate complexes of the form X—CH=CH—C(=O)—O–enzyme, where X is an unsaturated ring moiety, have provided exquisite structural and mechanistic detail on key catalytic groups in the active site.[1,2] These studies involve the serine protease group of enzymes where the alkoxy oxygen, —O—, forming a transient covalent link between the enzyme and the acyl group is from an active site serine. The α,β-unsaturated acyl group provides an ideal chromophoric label by which to generate the resonance Raman spectrum. It is important to extend these studies to the cysteine protease family of enzymes, *via* intermediates of the type X—CH=CH—C(=O)—S—enzyme, to investigate common mechanistic features.[3] Moreover, technical innovations now permit us to obtain high-quality Raman data for α,β-unsaturated esters bound to proteins for derivatives of coenzyme-A, *e.g.* $CH_3-CH=CH-CH=CH-C(=O)-S-CoA$ bound to crotonase.[5]

A factor which limits our interpretation of the Raman or resonance Raman spectra of the α,β-unsaturated thioesters, free in solution of bound to their target enzyme, is the paucity of information in the literature concerning the conformational and spectroscopic properties of these compounds. The present paper is the first in a series whose prupose is to fill that void. Despite their relevance, simple α,β-unsaturated carbonyl thioesters have not yet been the subject of any detailed structural and vibrational experimental study, at least in part because these compounds are considerably unstable and difficult to handle. In addition, to the best of our knowledge, no theoretical studies on this family of compounds have been undertaken until now. Thus, in the present study, the conformational preferences and vibrational properties of *cis*- and *trans*-*s*-ethyl thiocrotonate (abbreviated *c*-ETC and *t*-ETC) were studied by a combined *ab initio* SCF-MO calculation and vibrational spectroscopic approach, as a first step to the general understanding of the conformational and vibrational properties of α,β-unsaturated thioesters.

Experimental and Computational Methods

Synthesis and Equipment

0.74 ml (0.01 mol) ethanethiol and 1.39 ml (0.01 mol) triethylamine were combined in 50 ml dry CH_2Cl_2. The solution was stirred on an ice–water bath under nitrogen and 10 ml of dry CH_2Cl_2 containing 1 ml (0.01 mol) crotonyl chloride was added dropwise over 10 min. The solution was stirred for a further 15 min at room temperature and then extracted with 2 × 30 ml H_2O, 2 × 30 ml 0.1 mol l^{-1} sodium acetate pH 4, and 2 × 30 ml saturated aqueous NaCl. After drying the organic layer with dry Na_2CO_3, solvent was removed under vacuum. A sample of the remaining brown liquid was dissolved in hexane and purified by high-performance liquid chromatography (HPLC) on a silica column using hexane as eluent (3 ml min^{-1}). Peaks were detected using 220–260 nm absorbance and further analysed by UV, NMR, Raman and FTIR spectroscopies. For the NMR experiment peaks were combined, the hexane removed under vacuum, and samples redissolved in CD_3CN. The UV, Raman and FTIR studies were performed directly on the HPLC fractions in hexane or on the redissolved compounds in CD_3CN.

The HPLC column used for sample purification was a Supercosil LC-SI semiprep. 25.0 cm × 10 mm 5 μm pore silica column. UV spectra were obtained with a Cary 3 spectrometer (*t*-ETC: 217 and 263 nm, ratio of peak heights, 217/263 = 2.7; *c*-ETC: 221 and 266 nm, ratio of peak heights, 221/266 = 2.0). ^1H NMR spectra were obtained using a Varian Unity 400 NMR spectrometer operating at 400 MHz (*t*-ETC: δ 1.86 {dd, 1, *J* 2, 7 Hz}; 6.91 {dq, 1, *J* 7, 18 Hz}; 6.19 {dq, 1, *J* 2, 15 Hz}; 2.91 {*q*, 1, *J* 7 Hz}). FTIR spectra were obtained using a Digilab FTS 40A spectrometer equipped with a DTGS detector. Data collection was performed using a demountable liquid cell equipped with KBr windows. For each spectrum 64 scans were obtained and co-added. Raman spectra were obtained using a single monochromator, equipped with a CCD detector and s super notch filter. Data collection was performed using 90° sampling geometry with 300 mW 647.1 nm laser excitation. For each spectrum 20 scans each 10 s were acquired and co-added.

Computational Details

The *ab initio* SCF-MO calculations were carried out with the 6-31G* basis set[6] using the GAUSSIAN 92 program system[7] running on a VAX9000 computer. Molecular geometries were fully optimized by the force gradient method using Berny's algorithm.[8] The largest residual internal coordinate forces were always less than 3×10^{-4} E_h a_0^{-1} (1 E_h = 2625.5001 kJ mol^{-1}; 1 $a_0 = 5.29177 \times 10^{-11}$ m) or E_h rad^{-1}, for bond stretches and angle bends, respectively. The stopping criterion for the SCF iterative process required a density matrix convergence of less than 10^{-8}. The force constants (symmetry internal coordinates) to be used in the normal coordinate analysis were obtained from the *ab initio* Cartesian harmonic force constants using the program TRANSFORMER.[9] This program was also used to prepare the input data for the normal coordinate analysis programs used in this study (BUILD-G and VIBRAT[10]). The calculated force fields were scaled down by using a simple linear regression in order to adjust the calculated frequencies to the observed ones. Frequencies corresponding to unobserved or doubtfully assigned vibrations were then calculated from the *ab initio* force fields by interpolation using the straight line obtained previously. While very simple, this scaling procedure has the advantage, over more elaborate force-field scaling procedures which use several scale factors, of preserving the potential-energy distributions (PEDs) as they emerge from the *ab initio* calculations.

Results and Discussion

Geometries and Energies

Table 1 shows the 6-31G* energies and optimized geometries for the molecules studied. The atom numbering is presented in Fig. 1. As shown in our previous studies on thioesters and thioacids,[11–14] molecules having an *s-trans* conformation about the O=C—Y—R (Y = O or S; R = H or alkyl) axis have a much higher energy than those adopting an *s-cis* conformation about this axis ($\Delta E_{s\text{-}trans(C-Y)-s\text{-}cis(C-Y)} > 13$ kJ mol^{-1}) and thus were not considered in this study. From the results presented in Table 1, the following conclusions can be drawn:

(i) The energy of *c*-ETC is *ca.* 12 kJ mol^{-1} higher than that of *t*-ETC. This increase in energy in going from *t*-ETC to *c*-ETC can be ascribed to a reduced methyl–carbonyl distance in the latter molecule, which leads to steric strain. Indeed, this conclusion is reinforced by the relative values of the C—C=O, C=C—C(1), C(8)—C=C and C—C—H(16) bond angles in the two molecules, which are all larger in *c*-ETC owing to the methyl–carbonyl steric repulsion. Apart from the changes observed in the above bond angles (and in those which must adjust to compensate these changes), the structural differences between *t*-ETC and *c*-ETC are not significant.

(ii) The internal rotation about the C_α—C bond in *t*-ETC originates two different conformers: the *s-cis* and *s-trans* forms, with the C=C—C=O dihedral angle equal to 0 and 180°, respectively. For the isolated molecule, the *s-cis* form is *ca.* 7 kJ mol^{-1} more stable than the *s-trans* form. In *c*-ETC, only the *s-cis* conformation corresponds to a minimum in the potential-energy profile for internal rotation about the C_α—C bond, whilst the *s-trans*, conformation corresponds to a conformational transition state (*i.e.* to a saddle point having an energy of *ca.* 18 kJ mol^{-1} above the energy minimum). This different conformational behaviour found for *t*-ETC and *c*-ETC can be easily understood considering the relative importance of the steric interactions involving the β-carbon substituent *cis* to the C(=O)S fragment in the two molecules. When compared with the H atom [the β-carbon substituent *cis* to the C(=O)S fragment in *t*-ETC], the larger methyl substituent present in *c*-ETC leads to stronger steric repulsions with either the oxygen (in *s-cis* forms) or sulfur (in *s-trans*

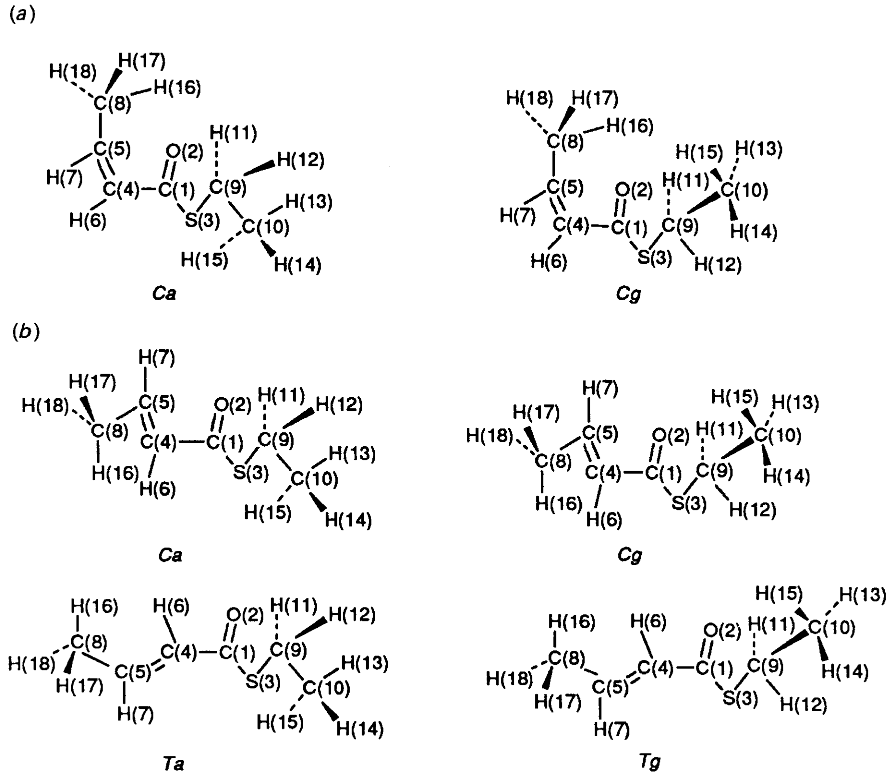

Fig. 1 Numbering of atoms for the relevant conformers on (*a*) *c*-ETC and (*b*) *t*-ETC

Table 1 6-31G* calculated optimized geometries, energies and electric dipole moments for the relevant forms of *c*-ETC and *t*-ETC

	c-ETC		*t*-ETC			
parameter	*Cg*	*Ca*	*Cg*	*Ca*	*Tg*	*Ta*
C=O	119.20	119.18	119.20	119.18	119.14	119.13
C(1)—S	178.62	178.49	178.24	178.08	178.95	178.75
C(1)—C(4)	148.47	148.50	148.42	148.45	148.43	148.44
C=C	132.80	132.79	132.36	132.35	132.29	132.27
C—H(6)	107.54	107.55	107.58	107.59	107.62	107.62
C—H(7)	107.88	107.89	107.67	107.67	107.71	107.73
C—C(8)	149.96	149.96	149.76	149.76	149.92	149.92
C—H(16)	107.63	107.63	108.33	108.33	108.31	108.31
C—H(17)	108.71	108.71	108.64	108.65	108.63	108.64
C—H(18)	108.71	108.71	108.64	108.65	108.63	108.64
S—C(9)	181.90	181.96	181.95	181.99	182.01	182.04
C—H(11)	108.02	108.04	108.02	108.04	107.98	108.01
C—H(12)	108.30	108.04	108.30	108.04	108.31	108.01
C(9)—C(10)	152.46	152.56	152.45	152.56	152.42	152.54
C—H(13)	108.63	108.49	108.63	108.49	108.63	108.49
C—H(14)	108.42	108.45	108.42	108.45	108.42	108.45
C—H(15)	108.22	108.45	108.22	108.45	108.21	108.45
O=C—S	121.79	121.45	122.42	122.08	121.49	121.18
C—C=O	126.00	126.10	124.25	124.33	120.90	121.00
C=C—C	126.00	126.01	120.44	120.46	126.12	126.10
H(6)—C—C	115.36	115.34	117.72	117.72	112.52	112.50
H(7)—C=C	115.77	115.79	117.88	117.85	119.85	119.82
C(8)—C=C	129.74	129.68	125.15	125.17	124.48	124.53
C—C(8)—H(16)	112.77	112.75	111.93	111.93	111.73	111.72
C—C(8)—H(17)	109.29	109.31	110.34	111.34	110.36	110.40
C—C(8)—H(18)	109.30	109.31	110.33	110.34	110.40	110.40
C—S—C	101.14	100.56	101.13	100.57	100.56	99.88
C(10)—C—S	113.96	109.94	113.94	109.95	114.05	106.70
H(11)—C—S	107.53	108.25	107.48	108.22	107.61	108.31
H(12)—C—S	104.83	108.25	104.84	108.22	104.51	108.31
C—C—H(13)	109.69	109.51	109.68	109.50	109.64	109.41
C—C—H(14)	111.20	111.48	111.20	109.48	111.20	111.51
C—C—H(15)	110.83	111.48	110.81	111.48	110.86	111.51
C—C=C—C	0.04	0.00	180.00	180.00	179.66	180.00
H—C=C—C(1)	180.03	180.00	0.01	0.00	− 0.14	0.00
C=C—C=O	− 0.34	0.00	− 0.11	0.00	− 175.81	180.00
H—C—C=O	179.73	180.00	179.92	180.00	3.58	0.00
C—C(=O)—S	180.37	180.00	− 179.65	180.00	− 179.33	180.00
O=C—S—C	0.99	0.00	0.93	0.00	2.71	0.00
C(1)—S—C—C	80.42	180.00	80.25	180.00	79.75	180.00
H(11)—C—S—C	− 43.17	58.00	− 43.27	58.30	− 44.05	58.38
H(12)—C—S—C	− 158.07	− 58.00	− 158.18	− 58.30	− 158.89	− 58.38
H(13)—C—C—S	178.39	180.00	178.51	180.00	178.19	180.00
H(14)—C—C—S	58.71	60.34	58.83	60.54	58.54	60.58
H(15)—C—C—S	− 62.25	− 60.34	− 62.15	− 60.55	− 62.49	− 60.58
H(16)—C—C=C	− 0.32	0.00	0.02	0.00	0.11	0.00
H(17)—C—C=C	121.39	121.75	121.02	120.99	121.00	120.90
H(18)—C—C=C	− 122.12	− 121.75	− 120.97	− 120.99	− 120.81	− 120.90
ΔE[a]	— (11.56)	1.394 (12.95)	—	1.501	7.181	8.502
$\lvert\mu\rvert$	1.140	1.034	1.459	1.370	2.209	2.226

Bond lengths in pm, angles in degrees, energies in kJ mol^{-1}, dipole moments in Debye (1 D = 3.335 64 × 10^{-30} C m); see Fig. 1 for atom numbering. [a] Energies relative to the most stable conformer; for *c*-ETC, the values presented in parentheses are energies relative to the most stable conformer of *t*-ETC. The total energy for the most stable form of *t*-ETC is −705.397 963 896 E_h.

conformations) atoms. This increase of energy due to the H → CH_3 substitution is, however, particularly critical for the *s-trans* conformation, where the steric interaction involves the sterically more important sulfur atom. Indeed, this interaction is strong enough to make planar *s-trans* conformation in *c*-ETC less stable than the non-planar structures about the C_α—C bond, despite the fact that a planar C=C—C=O axis leads to a more efficient overlap of the p(π) orbitals participating in the mesomerism associated with the C=C—C=O fragment.

(iii) The fundamental importance of the above-mentioned steric repulsions to the conformational preferences of the C=C—C=C axis in the studied molecules is reinforced by the calculated changes in the structural parameters associated with the *s-cis* → *s-trans* isomerization. Thus, in *t*-ETC, the C—C—S, C=C—C and H(7)—C=C angles increase considerably (*ca.* 4.2, 5.5 and 2.0°, respectively), whereas the C—C=O, O=C—S, H(6)—C—C, H(6)—C=C, C(8)—C=C and C(8)—C—H(7) angles decrease to compensate those changes. In turn, no significant changes are observed in the bond lengths, which usually are determined mainly by electronic effects.[11–14] In *c*-ETC, the structural differences between the stable *s-cis* conformation and the *s-trans* C=C—C=O axis (saddle point) follow identical patterns of variation [note that C(8)H_3 is now the β-carbon substituent *cis* to the C(=O)S fragment instead of H(7)]: the C—C—S, C=C—C and C(8)—C=C angles increase by *ca.* 8, 7 and 3°, these changes being compensated by those of C—C=O, O=C—S, H(6)—C—C, H(6)—C=C, H(7)—C=C and C(8)—C—H(7); in addition, the C—C(8)—H(16) angle increases by 2°.

(iv) Besides the forms resulting from internal rotation about the C_α—C axis, both *t*-ETC and *c*-ETC may exist in two different-by-symmetry stable conformations differing in the relative orientation of the terminal methyl group of the $S—CH_2CH_3$ fragment. The most stable of these conformations is a doubly degenerate conformational state (point group C_1), corresponding to C(1)—S—C—C axes of *ca.* ±80° (*gauche* forms). The second form is the C_S symmetric *anti* form [C(1)—S—C—C dihedral angle equals 180°], which is *ca.* 1.5 kJ mol^{-1} less stable than the *gauche* conformation in both *c*-ETC and *t*-ETC. In this latter molecule, the *anti-gauche* (C—S—C—C axis) relative energy does not depend on the relative orientation of the C=C—C=O axis). The fact that the conformation of the C—S—C—C axis is not significantly affected by the conformation of the acyl fragment is consonant with our previous studies on ethyl dithioacetate and ethyl dithiopropionate,[15,16] where the conformational preferences of this axis, in particular its trend to adopt *gauche* conformations, have been analysed in detail. The main structural changes associated with the *anti* → *gauche* rotamerization occur in the C(10)—C—S, H(11)—C—S and H(12)—C—S angles (*i.e.* those angles involving the atoms directly affected by the internal rotation), which increases by *ca.* 4° and decrease by *ca.* 1 and 4°, respectively, and follow the general trends reported in our previous studies on ethyl dithioesters.[15,16]

(v) The calculated electric dipole moments of the various conformers of *t*-ETC are larger than those of *c*-ETC. This result can be understood considering the closer proximity of the positively charged *β*-carbon methyl substituent of the negatively charged carbonyl oxygen in *c*-ETC. Indeed, this interpretation is reinforced by the considerably larger electric dipole moments found for the *s-trans* conformers of *t*-ETC, where these groups are optimally displaced from each other. On the other hand, the electric dipole moments associated with an *anti* or *gauche* C—S—C—C axis are very similar. Thus, it can be anticipated that the relative population about the *s-cis*/*s-trans* C=C—C=O axis must be sensitive to the polarity of the solvent, while the *gauche*/*anti* C—S—C—C axis population ratio will not vary significantly upon changing solvent polarity.

In summary, *c*-ETC exists as two different conformers, which has the C=C—C=O axis in the *s-cis* conformation and the C—S—C—C axis either in the *anti* or *gauche* conformations (*Ca* and *Cg* forms, see Fig. 1). In turn, *t*-ETC exists in four different conformational states differing by the relative orientation of the C=C—C=O and C—S—C—C axes; besides the *Ca* and *Cg* forms similar to those found for *c*-ETC, two different forms having the C=C—C=O axis in the *s-trans* conformation also participate in the conformational equilibrium (the *Ta* and *Tg* conformers, see Fig. 1). The different conformational behaviour between the two compounds is essentially determined by the presence of the strong repulsive steric interactions between the *β*-carbon methyl substituent and the sulfur atom in the *s-trans* C=C—C=O conformation of *c*-ETC, which considerably increase the energy of this conformation. Steric repulsions (this time involving the *β*-carbon methyl substituent and the carbonyl oxygen atom) are also the main factor which determine the relative energies of the most stable forms of *c*-ETC and *t*-ETC ($\Delta E_{(c\text{-ETC})-(t\text{-ETC})}$ = 12 kJ mol^{-1}). All these steric effects are reflected quite clearly in the structural parameters of the different molecules considered. Finally, considering the relative values of the dipole moments of the various conformers, the calculations indicate that solvent variation may be used successfully to change the C=C—C=O *s-cis*/*s-trans* relative populations, but does not provide a useful way to modify significantly the *anti*/*gauche* C—S—C—C conformational equilibrium.

Vibrational Studies

Both *c*-ETC and *t*-ETC molecules have 48 fundamental vibrations. In the case of the symmetric (C_S) conformers (*Ca*, *Ta*), the normal modes will span the irreducible representations 30A′ + 18A″, while those of the non-symmetric *gauche* forms (*Cg* and *Tg*, C_1 point group) belong to the A symmetry species. Hence, all vibrations are active in the IR. Table 2 presents the definition of the internal symmetry coordinates used in this study.

As mentioned in Experimental and Computational Methods, calculated spectra were obtained from the 6-31G* *ab initio* wavefunctions at the equilibrium geometries of the various conformers considered, and then adjusted to the observed frequencies by linear regression. In this adjustment, data related to the most stable conformers (*Cg*) of both *c*-ETC and *t*-ETC were used simultaneously (a total of 60 frequency values were used). As the calculated *vs.* experimental frequencies yielded a straight line ($\nu_{exp} = 0.8996\nu_{calc} - 14.4$) with a high correlation coefficient ($R^2 = 0.999279$), the calculated frequencies of these conformers were appropriately scaled (the mean and maximum errors in this scaling were 1.3% and 5.49%, respectively). The same frequency scaling was assumed for all the remaining conformers. Table 3–10 summarize the vibrational results of this study. The experimental and calculated spectra are presented in Fig. 2–4.

c-ETC

The FTIR spectrum of *c*-ETC in hexane solution (Fig. 2) is dominated by the intense bands at 1680 and 1014 cm^{-1}. These two bands are easily assigned to the ν(C=O) and ν(C_α—C) stretching modes, in agreement with the theoretical results, which also predict that these modes will be the most intense bands in the IR spectrum of this compound (Table 3). It should be noted, however, that the calculations overestimate the intensity of the ν(C_α—C) band and that, interestingly, the predicted intensity of the band due to the ν(C=C) stretching mode at *ca.* 1630 cm^{-1} is also consider-

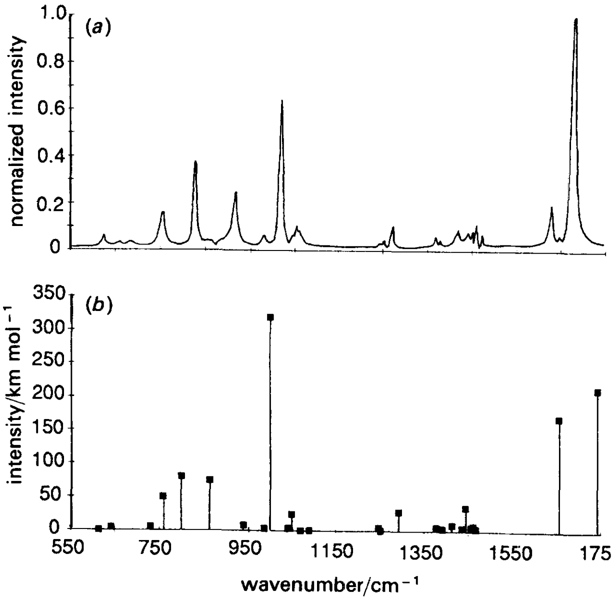

Fig. 2 FTIR spectrum (550–1750 cm^{-1} region) of *c*-ETC in hexane solution at room temperature (*a*) and 6-31G* calculated (*Cg*; scaled frequencies) IR spectrum (*b*)

Table 2 Definition of the internal symmetry coordinates used in the normal coordinate analysis[a]

	coordinate	symmetry[b]	definition
S_1	ν(C=O)	A′	ν(C=O)
S_2	ν(C—S)	A′	ν[C(1)—S]
S_3	ν(C$_\alpha$—C)	A′	ν[C(8)—C]
S_4	ν(C=C)	A′	ν(C=C)
S_5	ν(C$_\beta$—C)	A′	ν[C—C(8)]
S_6	ν(S—C)	A′	ν[S—C(10)]
S_7	ν(C—C)	A′	ν[C(9)—C(10)]
S_8	ν(C$_\alpha$—H)	A′	ν[C—H(6)]
S_9	ν(C$_\beta$—H)	A′	ν[C—H(7)]
S_{10}	ν(C$_\gamma$H$_3$)$_{as}$	A′	2ν[C—H(16)] – ν[C—H(17)] – ν[C—H(18)]
S_{11}	ν(C$_\gamma$H$_3$)$_{as}$	A″	ν[C—H(17)] – ν[C—H(18)]
S_{12}	ν(C$_\gamma$H$_3$)$_s$	A′	ν[C—H(16)] + ν[C—H(17)] + ν[C—H(18)]
S_{13}	ν(CH$_2$)$_{as}$	A″	ν[C—H(11)] – ν[C—H(12)]
S_{14}	ν(CH$_2$)$_s$	A′	ν[C—H(11)] + ν[C—H(12)]
S_{15}	ν(CH$_3$)$_{as}$	A′	2ν[C—H(13)] – ν[C—H(14)] – ν[C—H(15)]
S_{16}	ν(CH$_3$)$_{as}$	A″	ν[C—H(14)] – ν[C—H(15)]
S_{17}	ν(CH$_3$)$_s$	A′	ν[C—H(13) + ν[C—H(14)] + ν[C—H(15)]
S_{18}	δ(O=C—S)	A′	2δ(O=C—S) – δ[C—C=O) – δ[C(4)—C—S]
S_{19}	δ(C—C=O)	A′	δ(C—C=O) – δ[C(4)—C—S]
S_{20}	δ(C—S—C)	A′	δ(C—S—C)
S_{21}	δ(S—C—C)	A′	4δ[S—C—C(10)] – δ[S—C—H(11)] – δ[S—C—H(12)] – δ[C—C—H(11)] – δ[C—C—H(12)]
S_{22}	δ(C=C—C)	A′	2δ[C=C—C(1)] – δ[C=C—H(16)] – δ[C(1)—C—H(6)]
S_{23}	δ(C$_\alpha$—H)	A′	δ[C=C—H(16)] – δ[C(1)—C—H(6)]
S_{24}	δ(C—C=C)	A′	2δ[C(8)—C=C] – δ[C(8)—C—H(7)] – δ[C=C—H(7)]
S_{25}	δ(C$_\beta$—H)	A′	δ[C=C—H(7)] – δ[C(8)—C—H(7)]
S_{26}	δ(C$_\gamma$H$_3$)$_{as}$	A′	2δ[H(17)—C—H(18)] – δ[H(16)—C—H(17)] – δ[H(16)—C—H(18)]
S_{27}	δ(C$_\gamma$H$_3$)$_{as}$	A″	δ[H(16)—C—H(17)] – δ[H(16)—C—H(18)]
S_{28}	δ(C$_\gamma$H$_3$)$_s$	A′	δ[H(17)—C—H(18)] + δ[H(16)—C—H(17)] + δ[H(16)—C—H(18)] – δ[C—C—H(16)] – δ[C—C—H(17)] – δ[C—C—H(18)]
S_{29}	δ(CH$_3$)$_{as}$	A′	2δ[H(14)—C—H(15)] – δ[H(13)—C—H(14)] – δ[H(13)—C—H(15)]
S_{30}	δ(CH$_3$)$_{as}$	A″	δ[H(13)—C—H(14)] – δ[H(13)—C—H(15)]
S_{31}	δ(CH$_3$)$_s$	A′	δ[H(14)—C—H(15)] + δ[H(13)—C—H(14)] + δ[H(13)—C—H(15)] – δ[C—C—H(13)] – δ[C—C—H(14)] – δ[C—C—H(15)]
S_{32}	δ(CH$_2$)	A′	5δ[H(11)—C—H(12)] – δ[S—C—C(10)] – δ[S—C—H(11)] – δ[S—C—H(12)] – δ[C—C—H(11)] – δ[C—C—H(12)]
S_{33}	ω(CH$_2$)	A′	δ[S—C—H(11)] + δ[S—C—H(12)] – δ[C—C—H(11)] – δ(C—C—H(12)]
S_{34}	tw(CH$_2$)	A″	δ[S—C—H(11)] – δ[S—C—H(12)] – δ[C—C—H(11)] + δ[C—C—H(12)]
S_{35}	γ(CH$_2$)	A″	δ[S—C—H(11)] – δ[S—C—H(12)] + δ[C—C—H(11)] – δ[C—C—H(12)]
S_{36}	γ(C$_\gamma$H$_3$)	A′	2δ[C—C—H(16)] – δ[C—C—H(17)] – δ[C—C—H(18)]
S_{37}	γ(C$_\gamma$H$_3$)	A″	δ[C—C—H(17)]–δ[C—C—H(18)]
S_{38}	γ(CH$_3$)	A′	2δ[C—C—H(13)] – δ[C—C—H(14)] – δ[C—C—H(15)]
S_{39}	γ(CH$_3$)	A″	δ[C—C—H(14)] – δ[C—C—H(15)]
S_{40}	γ(C=O)	A″	Ω[C—C(=O)—C]
S_{41}	γ(C$_\alpha$—H)	A″	Ω\{C=C[—H(6)]—C\}
S_{42}	γ(C$_\beta$—H)	A″	Ω\{C—C[—H(7)]=C\}
S_{43}	τ(C=C)	A″	τ(C—C=C—C)
S_{44}	τ(C$_\alpha$—C)	A″	τ(C=C—C=O)
S_{45}	τ(C—S)	A″	τ(O=C—S—C)
S_{46}	τ(S—C)	A″	τ[C—S—C—C(10)]
S_{47}	τ(C$_\gamma$H$_3$)	A″	τ[C=C—C—H(16)] + τ[C=C—C—H(17)] + τ[C=C—C—H(18)]
S_{48}	τ(CH$_3$)	A″	τ[S—C—C—H(13)] + τ[S—C—C—H(14)] + τ[S—C—C—H(15)]

[a] Normalization constants are not given here; they are chosen as $N = (\Sigma c_i^2)^{-1/2}$, where c_i are the coefficients of the individual valence coordinates; ν, bond stretching; δ, bending, γ, rocking, ω, wagging, tw, twisting, τ, torsion, Ω, out-of-plane deformation. See Fig. 1 for atom numbering. [b] Symmetry of coordinates taken as reference the symmetric (C_s) conformers. In the case of the non-symmetric C_1 forms, all coordinates belong to the A representation.

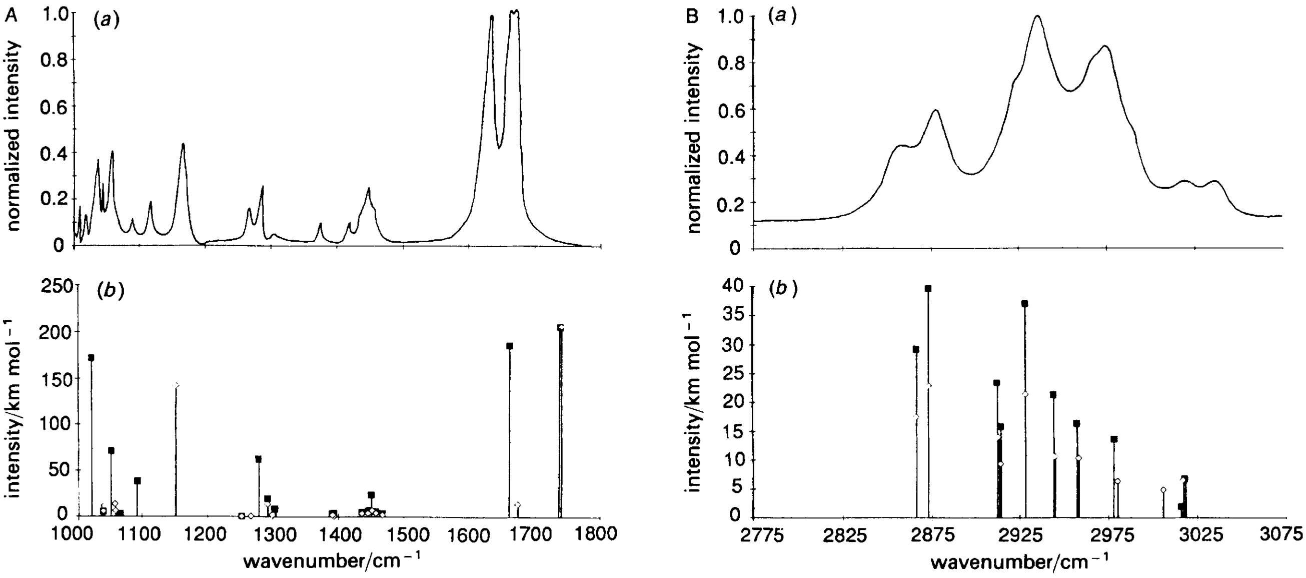

Fig. 3 A, FTIR spectrum (1000–1800 cm^{-1} region) of *t*-ETC in CD$_3$CN solution at room temperature (*a*) and 6-31G* calculated (*Cg* and *Tg*; scaled frequencies) IR spectrum (*b*). ■, *s-cis*; ◇, *s-trans*. The calculated intensities of the bands due to the *s-trans* conformer are multiplied by the factor 1/1.70 (see text). B, FTIR spectrum (2775–3075 cm^{-1} region) of *t*-ETC in CD$_3$CN solution at room temperature (*a*) and 6-31G* calculated (*Cg* and *Tg*; scaled frequencies) IR spectrum (*b*). ■, *s-cis*; ◇, *s-trans*. The calculated intensities of the bands due to the *s-trans* conformer are multiplied by the factor 1/1.70 (see text).

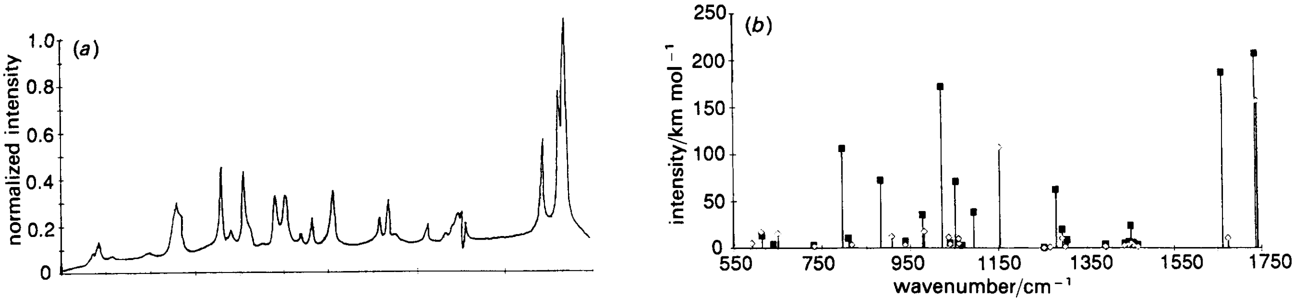

Fig. 4 FTIR spectrum (550–1750 cm^{-1} region) of *t*-ETC in hexane solution at room temperature (*a*) and 6-31G* calculated (*Cg* and *Tg*; scaled frequencies) IR spectrum (*b*). ■, *s-cis*; ◇, *s-trans*. The calculated intensities of the bands due to the *s-trans* conformer are multiplied by the factor 1/2.25 (see text).

Table 3 Experimental frequencies and calculated frequencies and intensities for *c*-ETC[a]

approximate description	calculated						experimental[b] FTIR (in hexane solution)
	Cg			*Ca*			
	ab initio	scaled	intensity	*ab initio*	scaled	intensity	
$\nu(C_\gamma H_3)_{as}$	3377	3024	4.6	3377	3024	4.4	
$\nu(C_\alpha{-}H)$	3369	3016	6.1	3368	3016	6.8	
$\nu(CH_2)_{as}$	3325	2977	18.1	3328	2979	16.1	
$\nu(C_\beta{-}H)$	3325	2977	17.8	3324	2976	22.1	
$\nu(CH_3)_{as}$	3302	2956	17.0	3282	2938	45.3	
$\nu(CH_3)_{as}$	3271	2928	33.7	3279	2938	21.6	
$\nu(CH_2)_s$	3254	2912	15.7	3268	2926	0.4	
$\nu(C_\gamma H_3)_{as}$	3242	2902	26.6	3242	2902	27.0	
$\nu(CH_3)_s$	3210	2873	39.8	3212	2875	34.5	
$\nu(C_\gamma H_3)_s$	3200	2864	30.0	3200	2864	30.9	
$\nu(C{=}O)$	*1951*	1741	214.0	1952	1741	235.5	1680
$\nu(C{=}C)$	*1855*	1654	170.5	1856	1655	167.8	1627
$\delta(CH_3)_{as}$	*1647*	1467	3.5	1646	1466	2.0	1470
$\delta(C_\gamma H_3)_{as}$	*1641*	1462	7.7	1642	1643	7.8	1457
$\delta(CH_3)_{as}$	*1636*	1457	5.4	1640	1461	6.5	1449
$\delta(C_\gamma H_3)_{as}$	*1621*	1444	35.7	1621	1444	33.9	1436
$\delta(CH_2)$	*1612*	1436	4.6	1629	1451	8.8	1417 (*Cg*), 1436 (*Ca*)
$\delta(C_\alpha{-}H)$	*1587*	1413	9.4	1587	1413	9.0	1411
$\delta(CH_3)_s$	*1562*	1391	3.4	1567	1395	1.6	1375
$\delta C_\gamma H_3)_s$	*1547*	1377	5.8	1547	1377	5.9	1365
$\omega(CH_2)$	*1452*	1292	28.6	1445	1286	31.3	1267
$tw(CH_2)$	*1408*	1252	0.2	1384	1231	0.0	1248 (*Cg*), 1239 (*Ca*)
$\delta(C_\beta{-}H)$	1402	1247	4.7	1402	1247	4.6	1248
$\gamma(C_\gamma H_3)$	*1226*	1088	0.8	1225	1088	0.7	1072
$\gamma(C_\gamma H_3)$	*1203*	1068	0.1	1203	1068	0.1	1056
$\gamma(CH_3)$	*1180*	1047	24.9	1176	1043	41.0	1050
$\gamma(CH_3)$	*1171*	1039	3.4	1164	1033	0.1	1043
$\nu(C_\alpha{-}C)$	*1125*	998	319.7	1127	999	317.7	1014
$\gamma(C_\alpha{-}H)$	1110	984	2.9	1110	984	2.8	—
$\nu(C{-}C)$	*1059*	938	7.8	1064	943	8.1	974
$\nu(C_\beta{-}C)$	*973*	861	74.5	973	861	74.6	911
$\nu(C{-}S)$	*903*	798	79.9	903	798	84.4	822
$\gamma(C_\beta{-}H)$	*859*	758	49.9	860	759	41.2	750
$\gamma(CH_2)$	828	730	4.9	849	749	12.2	—
$\nu(S{-}C)$	*730*	642	4.1	755	665	1.6	655 (*Cg*), 680 (*Ca*)
$\gamma(C{=}O)$	*697*	613	0.1	696	612	0.0	620
$\delta(C{-}C{=}C)$	581	508	1.6	602	527	1.6	
$\delta(O{=}C{-}S)$	491	427	3.6	484	421	3.9	
$\delta(S{-}C{-}C)$	385	332	2.4	362	311	5.2	
$\tau(C{=}C)$	357	307	1.4	361	310	1.4	
$\tau(CH_3)$	307	262	7.0	264	223	0.2	
$\delta C{-}C{=}O)$	297	253	4.4	298	253	3.6	
$\delta(C{=}C{-}C)$	244	205	3.0	249	210	5.1	
$\delta(C{-}S{-}C)$	163	132	1.3	120	93	1.9	
$\tau C_\gamma H_3)$	117	91	0.0	120	93	0.5	
$\tau(S{-}C)$	93	69	0.9	56	36	0.0	
$\tau(C{-}S)$	77	55	3.5	97	73	4.2	
$\tau(C_\alpha{-}C)$	33	15	0.9	31	13	1.2	

[a] Frequencies in cm^{-1}. Intensities in km mol^{-1}, ν, bond stretching; δ, bending, γ rocking, ω, wagging, tw, twisting, τ, torsion, see Table 2 for definition of symmetry coordinates. Frequencies in italic were those used for force filed scaling. [b] Except in the cases explicitly indicated in the Table, all observed bands are considered to have contributions from both *Cg* and *Ca* conformers.

Table 4 Normal coordinate analysis for *c*-ETC (form *Cg*)[a]

approximate description	calculated frequency	PED[b]
$\nu(C_\gamma H_3)_{as}$	3377	$S_{10}(79) + S_{12}(11)$
$\nu(C_\alpha{-}H)$	3369	$S_8(88)$
$\nu(CH_2)_{as}$	3325	$S_{13}(57) + S_9(24) + S_{16}(12)$
$\nu(C_\beta{-}H)$	3325	$S_9(67) + S_{13}(20)$
$\nu(CH_3)_{as}$	3302	$S_{16}(66) + S_{15}(15) + S_{13}(11)$
$\nu(CH_3)_{as}$	3271	$S_{15}(73) + S_{16}(18)$
$\nu(CH_2)_s$	3254	$S_{14}(84)$
$\nu(C_\gamma H_3)_{as}$	3242	$S_{11}(101)$
$\nu(CH_3)_s$	3210	$S_{17}(93)$
$\nu(C_\gamma H_3)_s$	3200	$S_{12}(87) + S_{10}(16)$
$\nu(C{=}O)$	1951	$S_1(94)$
$\nu(C{=}C)$	1855	$S_4(76) + S_{25}(10)$
$\delta(CH_3)_{as}$	1647	$S_{29}(69) + S_{30}(24)$
$\delta C_\gamma H_3)_{as}$	1641	$S_{27}(89)$
$\delta(CH_3)_{as}$	1636	$S_{30}(76) + S_{29}(22)$
$\delta(C_\gamma H_3)_{as}$	1621	$S_{26}(87)$
$\delta(CH_2)$	1612	$S_{32}(109)$
$\delta(C_\alpha{-}H)$	1587	$S_{23}(34) + S_{25}(26) + S_{28}(20) + S_{26}(13) + S_5(10)$
$\delta(CH_3)_s$	1562	$S_{31}(103)$
$\delta(C_\gamma H_3)_s$	1547	$S_{28}(83) + S_{25}(12) + S_{23}(11)$
$\omega(CH_2)$	1452	$S_{33}(91)$
$tw(CH_2)$	1408	$S_{34}(65) + S_{39}(17)$
$\delta(C_\beta{-}H)$	1402	$S_{25}(38) + S_{23}(28)$
$\gamma(C_\gamma H_3)$	1226	$S_{36}(48) + S_{24}(16) + S_5(11)$
$\gamma(C_\gamma H)_3)$	1203	$S_{42}(48) + S_{37}(43)$
$\gamma(CH_3)$	1180	$S_{39}(27) + S_{34}(21) + S_{35}(16) + S_{38}(11)$
$\gamma(CH_3)$	1171	$S_{38}(44) + S_\gamma(20)$
$\nu(C_\alpha{-}C)$	1125	$S_3(46) + S_{18}(20) + S_2(19)$
$\gamma(C_\alpha{-}H)$	1110	$S_{41}(43) + S_{37}(27) + S_{42}(18)$
$\nu(C{-}C)$	1059	$S_7(63) + S_{38}(20)$
$\nu(C_\beta{-}C)$	973	$S_5(58) + S_{36}(19)$
$\nu(C{-}S)$	903	$S_{22}(40) + S_{19}(24) + S_2(13) + S_3(12) + S_{36}(11)$
$\gamma(C_\beta{-}H)$	859	$S_{40}(30) + S_{42}(22) + S_{43}(14)$
$\gamma(CH_2)$	828	$S_{35}(68) + S_{40}(38)$
$\nu(S{-}C)$	730	$S_6(88)$
$\gamma(C{=}O)$	697	$S_{40}(58) + S_{42}(41) + S_{43}(28) + S_{27}(12)$
$\delta(C{-}C{=}C)$	581	$S_2(56) + S_{24}(24)$
$\delta(O{=}C{-}S)$	491	$S_{18}(42) + S_{24}(30) + S_3(14)$
$\delta(S{-}C{-}C)$	385	$S_{21}(48) + S_{43}(31)$
$\tau(C{=}C)$	357	$S_{43}(60) + S_{41}(15)$
$\tau(CH_3)$	307	$S_{48}(37) + S_{20}(27)$
$\delta(C{-}C{=}O)$	297	$S_{19}(28) + S_{24}(24) + S_{21}(15)$
$\delta(C{=}C{-}C)$	244	$S_{48}(56) + S_{22}(18) + S_{20}(11)$
$\delta(C{-}S{-}C)$	163	$S_{20}(29) + S_{19}(22) + S_{22}(18) + S_{46}(17) + S_{48}(11)$
$\tau(C_\gamma H_3)$	117	$S_{47}(97)$
$\tau(S{-}C)$	93	$S_{46}(79)$
$\tau(C{-}S)$	77	$S_{45}(84) + S_{47}(11)$
$\tau(C_\alpha{-}C)$	33	$S_{44}(85)$

[a] Frequencies in cm^{-1}. ν, bond stretching; δ, bending, γ, rocking, ω, wagging, tw, twisting, τ, torsion, see Table 2 for definition of symmetry coordinate. [b] Only PED values greater than 10% are given.

ably overestimated by the calculations. Since the C=C and C_α—C bonds are interacting by mesomerism and the extension of this effect certainly contributes significantly to the relative polarity of these two bonds[17–19] these results may be related, and they may indicate that the basis set used in the calculations may have some limitations in describing precisely the electron distribution in this fragment. The difference between the experimental and calculated intensities of the ν(C=C) and $\nu(C_\alpha$—C) bands could also have been ascribed to solute–solvent interactions, but these interactions should then also affect significantly the intensity of ν(C=O), and this is not in agreement with the observations. Apart from the foregoing point, the general agreement between the calculated and experimental spectrum of *c*-ETC (both frequencies and intensities) is remarkable (see Fig. 2 and Table 3). As the energy difference between the two conformers of this compound (*Cg* and *Ca*) is predicted to be small (*ca.* 1.4 kJ mol^{-1}), both conformers are present in significant amounts at room temperature and they must both contribute to the observed spectrum. However, since besides being more stable the *Cg* form is doubly degenerate, it must provide the main contribution to the bands observed. The following additional points, resulting either from the comparison between the experimental and calculated spectra or from the normal coordinate analysis data (Tables 4 and 5) are of note:

(i) Above 600 cm^{-1}, the frequencies calculated for the *Ca* and *Cg* forms are, in general, very similar. Thus, few band splittings can be seen in the spectrum. However, the $\delta(CH_2)$, $tw(CH_2)$, $\gamma(CH_2)$ and ν(S=C) modes are calculated to have considerably different frequencies in the two forms and should, in principle, give rise to observable doublets. Unfortunately, only four bands can be ascribed to a single conformer, and all of these are either very weak or partially overlapped bands: 655 cm^{-1} [ν(S—C) *Cg*], 680 cm^{-1} [ν(S—C) *Ca*], 1239 cm^{-1} [$tw(CH_2)$ *Ca*] and 1417 cm^{-1} [$\delta(CH_2)$ *Cg*]; the remaining bands are superimposed with bands due to other vibrations [$\delta(CH_2)$ *Ca* contributes to the band at 1436 cm^{-1}, assigned to $\delta(C_\gamma H_3)_{as}$; $tw(CH_2)$ *Cg* con-

Table 5 Normal coordinate analysis for *c*-ETC (form *Ca*)[a]

approximate description		calculated frequency	PED[b]
$\nu(C_\gamma H_3)_{as}$	A′	3377	$S_{10}(79) + S_{12}(11)$
$\nu(C_\alpha{-}H)$	A′	3368	$S_8(88)$
$\nu(CH_2)_{as}$	A″	3328	$S_{13}(95)$
$\nu(C_\beta{-}H)$	A′	3324	$S_9(90)$
$\nu(CH_3)_{as}$	A′	3282	$S_{15}(68) + S_{14}(33)$
$\nu(CH_3)_{as}$	A″	3279	$S_{16}(96)$
$\nu(CH_2)_s$	A′	3268	$S_{14}(68) + S_{15}(33)$
$\nu(C_\gamma H_3)_{as}$	A″	3242	$S_{11}(101)$
$\nu(CH_3)_s$	A′	3212	$S_{17}(100)$
$\nu(C_\gamma H_3)_s$	A′	3200	$S_{12}(88) + S_{10}(16)$
$\nu(C{=}O)$	A′	1952	$S_1(94)$
$\nu(C{=}C)$	A′	1856	$S_4(76) + S_{25}(10)$
$\delta(CH_3)_{as}$	A′	1646	$S_{29}(86)$
$\delta(C_\gamma H_3)_{as}$	A″	1642	$S_{27}(89)$
$\delta(CH_3)_{as}$	A″	1640	$S_{30}(100)$
$\delta(C_\gamma H_3)_{as}$	A′	1629	$S_{32}(98)$
$\delta(CH_2)$	A′	1621	$S_{26}(87)$
$\delta(C_\alpha{-}H)$	A′	1587	$S_{23}(34) + S_{25}(25) + S_{28}(20) + S_{26}(13) + S_5(10)$
$\delta(CH_3)_s$	A′	1567	$S_{31}(105)$
$\delta C_\gamma H_3)_s$	A′	1547	$S_{28}(83) + S_{25}(12) + S_{23}(11)$
$\omega(CH_2)$	A′	1445	$S_{33}(92)$
tw(CH_2)	*A′*	1402	$S_{25}(38) + S_{23}(28) + S_4(10)$
$\delta(C_\beta{-}H)$	A″	1384	$S_{34}(56) + S_{39}(22)$
$\gamma(C_\gamma H_3)$	A′	1225	$S_{36}(48) + S_{24}(16) + S_5(11)$
$\gamma(C_\gamma H_3)$	A″	1203	$S_{42}(47) + S_{37}(44)$
$\gamma(CH_3)$	A′	1164	$S_{38}(53) + S_7(21)$
$\gamma(CH_3)$	A″	1176	$S_{34}(39) + S_{39}(32) + S_{35}(16)$
$\nu(C_\alpha{-}C)$	A′	1127	$S_3(46) + S_{18}(20) + S_2(19)$
$\gamma(C_\alpha{-}H)$	A″	1110	$S_{41}(43) + S_{37}(27) + S_{42}(18)$
$\nu(C{-}C)$	A′	1064	$S_7(67) + S_{38}(15)$
$\nu(C_\beta{-}C)$	A′	973	$S_5(58) + S_{36}(19)$
$\nu(C{-}S)$	A′	903	$S_{22}(40) + S_{19}(24) + S_2(13) + S_3(12) + S_{36}(11)$
$\gamma(C_\beta{-}H)$	A″	860	$S_{40}(29) + S_{42}(20) + S_{43}(13)$
$\gamma(CH_2)$	A″	849	$S_{35}(68) + S_{39}(39)$
$\nu(S{-}C)$	A′	755	$S_6(85) + S_{38}(10)$
$\gamma(C{=}O)$	A″	696	$S_{40}(57) + S_{42}(42) + S_{43}(28) + S_{27}(13)$
$\delta(C{-}C{=}C)$	A′	602	$S_2(54) + S_{24}(20)$
$\delta(O{=}C{-}S)$	A′	484	$S_{18}(41) + S_{24}(38) + S_3(14) + S_{22}(10)$
$\delta(S{-}C{-}C)$	A′	362	$S_{21}(52) + S_{18}(13) + S_{24}(13) + S_{19}(12)$
$\tau(C{=}C)$	A″	361	$S_{43}(75) + S_{41}(16) + S_{42}(10)$
$\tau(CH_3)$	A′	298	$S_{19}(35) + S_{20}(18) + S_{24}(12) + S_2(11)$
$\delta C{-}C{=}O)$	A″	264	$S_{48}(100)$
$\delta(C{=}C{-}C)$	A′	249	$S_{22}(35) + S_{21}(20) + S_{20}(14) + S_{24}(14)$
$\delta(C{-}S{-}C)$	A′	120	$S_{20}(53) + S_{19}(23) + S_{21}(14) + S_{18}(13) + S_{22}(12)$
$\tau C_\gamma H_3)$	A″	120	$S_{47}(82) + S_{45}(21)$
$\tau(C{-}S)$	A″	97	$S_{45}(58) + S_{47}(21)$
$\tau(S{-}C)$	A″	56	$S_{46}(86) + S_{44}(27)$
$\tau(C_\alpha{-}C)$	A″	31	$S_{44}(78) + S_{46}(25)$

[a] Frequencies in cm^{-1}. ν, bond stretching; δ, bending, γ, rocking, ω, wagging, tw, twisting, τ, torsion, see Table 2 for definition of symmetry coordinates. [b] Only PED values greater than 10% are given.

tributes to the band at 1248 cm^{-1}, assigned to $\delta(C_\beta{-}H)$, $\gamma(CH_2)$ *Ca* and *Cg* are probably underneath the intense band at 750 cm^{-1}, due to the $\gamma(C_\beta{-}H)$ vibration].

(ii) The experimental frequencies of $\nu(C{=}C)$ and, in particular, of $\nu(C{=}O)$ are significantly smaller than the calculated (scaled) values. These results are consonant with a slightly increased polarity of these bonds (less double-bond character) due to weak interactions with the solvent.

(iii) The S—C stretching coordinate does not mix very much with any other coordinate, thus giving rise to essentially pure vibrations in both *Ca* and *Cg* forms. On the other hand, both $C_\alpha{-}C$ and C—S coordinates are considerably mixed with each other and with other oscillators: $\nu(C_\alpha{-}C)$ mixes mainly with $\nu(C{-}S)$ and $\delta(O{=}C{-}S)$; $\nu(C{-}S)$ with $\nu(C_\alpha{-}C)$ and a series of bending coordinates [$\delta(C{=}C{-}C)$, $\delta(C{-}C{=}C)$, $\delta(C{-}C{=}O)$]. Indeed, though $\nu(C{-}S)$ is here assigned to the intense band at 822 cm^{-1} (calculated, 798 cm^{-1}), the normal mode analysis yields greater PED values for this coordinate associated with the calculated bands at 508 cm^{-1} (*Cg*) and 527 cm^{-1} (*Ca*), here ascribed to $\delta(C{-}C{=}C)$. While it can be concluded that in this kind of molecules $\nu(C{-}S)$ is definitely not a well localized vibration, the assignment of the 822 cm^{-1} band to $\nu(C{-}S)$ is justified for two main reasons: first, its relatively high intensity [$\nu(C{-}S)$ is generally an intense band in the IR];[15,16] secondly, because it can be expected that, owing to an increased partial double-bond character of the C—S bond when compared with the S—C bond, due to mesomerism involving the C(=O)S fragment, the frequency of the stretching vibration associated with this bond will be higher than that of $\nu(S{-}C)$.

t-ETC

In the case of *t*-ETC, contributions to the vibrational spectra are expected from all four conformers (*Cg*, *Ca*, *Tg*, *Ta*). As for *c*-ETC, the calculated spectra of forms differing in the relative orientation of the C—S—C—C axis do not differ very much, and thus only a few bands may be ascribed to individual conformers differing in the relative orientation of

Table 6 Experimental frequencies and calculated frequencies and intensities for *t*-ETC[a]

approximate description	calculated												experimental (FTIR)[b]	
	Cg			*Ca*			*Tg*			*Ta*			(in hexane solution)	(in D$_3$CN solution)
	ab initio	scaled	intensity	*ab initio*	scaled	intensity	*ab initio*	scaled	intensity	*ab initio*	scaled	intensity		
$\nu(C_\beta{-}H)$	***3371***	3018	6.8	**3370**	3017	6.7	**3358**	3006	8.3	**3356**	3005	9.8		3037^c
$\nu(C_\alpha{-}H)$	***3368***	3016	1.9	**3367**	3015	2.5	**3370**	3017	11.2	**3369**	3016	11.4		3019^c
$\nu(CH_2)_{as}$	***3326***	2978	13.7	**3328**	2979	15.6	**3329**	2980	10.9	**3332**	2983	14.7		2991^c
$\nu(CH_3)_{as}$	***3303***	2957	16.4	**3288**	2944	21.6	**3304**	2958	17.7	**3283**	2939	45.2		2976^c (*Cg*), 2961^c (*Ca*)
$\nu(C_\gamma H_3)_{as}$	***3288***	2944	21.4	**3282**	2938	45.4	**3290**	2945	18.1	**3290**	2945	17.7		2961^c
$\nu(CH_3)_{as}$	***3271***	2928	37.1	**3279**	2935	22.0	**3271**	2928	36.6	**3279**	2935	22.8		2937^c
$\nu(CH_2)_s$	***3255***	2914	15.9	**3268**	2925	0.4	**3255**	2914	15.9	**3270**	2927	0.5		2924^c
$\nu(C_\gamma H_3)_{as}$	***3253***	2912	23.5	**3253**	2912	33.7	**3254**	2913	23.8	**3254**	2913	24.1		2924^c
$\nu(CH_3)_s$	***3210***	2873	39.7	**3212**	2875	34.1	**3210**	2873	39.0	**3212**	2875	32.0		2878^c
$\nu(C_\gamma H_3)_s$	***3202***	2866	29.2	**3200**	2864	29.6	**3202**	2866	29.8	**3202**	2866	29.6		2858^c
$\nu(C{=}O)$	***1949***	1739	206.3	**1951**	1741	226.6	**1951**	1741	352.0	**1953**	1742	367.1	1683, 1675*	1672, 1666*
$\nu(C{=}C)$	***1864***	1662	186.4	**1865**	1663	180.2	**1877**	1674	23.8	**1878**	1675	23.5	1664	1636
$\delta(CH_3)_{as}$	***1647***	1467	3.5	**1646**	1466	1.9	**1647**	1467	3.5	**1646**	1466	1.8	1462	1556
$\delta(CH_3)_{as}$	***1636***	1457	5.9	**1640**	1461	6.4	**1636**	1457	6.6	**1640**	1461	6.5	1462	1456
$\delta(C_\gamma H_3)_{as}$	***1628***	1450	23.8	**1628**	1450	29.1	**1629**	1451	12.2	**1629**	1451	11.9	1445	1447
$\delta(C_\gamma H_3)_{as}$	***1623***	1446	6.6	**1623**	1446	6.6	**1622**	1445	7.0	**1622**	1445	7.0	1430	1438
$\delta(CH_2)$	***1612***	1436	4.9	**1629**	1451	3.3	**1612**	1436	5.9	**1629**	1451	7.8	1416 (*Cg*), 1430 (*Ca*)	1419 (*Cg*), 1438 (*Ca*)
$\delta(C_\gamma H_3)_s$	***1564***	1393	4.1	**1564**	1393	4.1	**1565**	1393	1.7	**1565**	1393	2.0	1375	1378
$\delta(CH_3)_s$	***1562***	1391	3.5	**1467**	1305	2.1	**1562**	1391	3.8	**1467**	1305	1.8	1375 (*Cg*), 1300 (*Ca*)	1378 (*Cg*), 1304 (*Ca*)
$\delta(C_\alpha{-}H)$	***1464***	1303	8.4	**1465**	1304	5.0	**1423**	1266	1.6	**1422**	1265	0.4	1300	1304
$\omega(CH_2)$	***1452***	1292	19.6	**1445**	1286	18.8	**1452**	1292	23.3	**1446**	1286	21.9	1267^c	1269^c
$\delta(C_\beta{-}H)$	***1437***	1278	62.2	**1437**	1278	74.7	**1460**	1299	2.9	**1461**	1300	2.3	1286	1287
tw(CH_2)	**1408**	1252	0.4	**1384**	1231	0.0	**1408**	1252	0.6	**1384**	1231	0.0	—	
$\gamma(C_\gamma H_3)$	***1231***	1093	38.1	**1231**	1093	40.9	**1194**	1060	11.0	1193	1059	2.6	1116	1120
$\gamma(C_\gamma H_3)$	***1201***	1066	3.0	**1201**	1066	3.0	**1193**	1059	23.4	**1191**	1057	58.3	1089^c	1092^c
$\gamma(CH_3)$	***1187***	1053	71.0	**1182**	1049	110.8	**1172**	1040	10.0	**1170**	1038	5.0	1054^c	1060^c
$\gamma(CH_3)$	***1172***	1040	5.3	**1164**	1033	0.2	**1169**	1037	26.6	**1164**	1033	0.1	1054^c	1060^c
$\nu(C_\alpha{-}C)$	***1152***	1022	171.9	**1155**	1025	114.2	**1298**	1153	241.8	**1299**	1154	262.0	1035, 1163*	1039, 1167*
$\gamma(C_\alpha{-}H)$	***1102***	977	35.1	**1102**	977	35.1	**1107**	981	39.4	**1107**	981	39.4	962, 974*	
$\nu(C{-}C)$	***1059***	938	7.2	**1064**	943	6.4	**1059**	938	7.2	**1064**	943	6.7	934^d	
$\nu(C_\beta{-}C)$	***996***	882	71.4	**996**	882	70.9	**1024**	907	27.4	**1024**	907	27.6	911^e	
$\gamma(C_\beta{-}H)$	***915***	809	10.3	**916**	810	10.2	**923**	816	7.0	**923**	816	6.5	822	
$\nu(C{-}S)$	***901***	796	106.0	903	798	109.5	**696**	612	39.1	**708**	622	57.1	810^f	
$\gamma(CH_2)$	***829***	731	2.8	**850**	750	2.0	**831**	733	4.3	**851**	751	2.2	751	
$\nu(S{-}C)$	***728***	640	3.8	**755**	665	0.9	**739**	650	35.4	**763**	672	16.4	635 (*Cg*)^g, 661 (*Ca*)^h	
$\gamma(C{=}O)$	***698***	614	13.3	**697**	613	14.3	**673**	591	12.4	**674**	592	12.6	620^i	
$\delta(O{=}C{-}S)$	**557**	487	0.2	575	503	0.4	**609**	533	2.5	**610**	534	4.4		
$\delta(C{-}C{=}C)$	**439**	381	7.1	**436**	378	6.0	**330**	282	6.0	**326**	279	0.7		
$\delta(S{-}C{-}C)$	**392**	338	2.4	**313**	267	1.4	**387**	334	0.4	**363**	312	5.8		
$\delta(C{=}C{-}C)$	**333**	285	8.1	**378**	326	9.2	**150**	120	0.8	**210**	174	6.3		
$\tau(CH_3)$	**295**	251	2.1	**265**	224	0.3	**297**	253	3.7	**265**	224	0.3		
$\tau(C{=}C)$	**226**	189	1.5	**225**	188	0.3	**197**	163	0.1	**197**	163	0.1		
$\delta(C{-}S{-}C)$	**221**	184	1.6	**219**	183	3.8	**214**	178	2.4	**115**	89	1.5		
$\tau(C_\gamma H_3)$	**211**	175	0.6	**212**	176	0.8	**220**	184	3.0	**218**	182	1.2		
$\delta(C{-}C{=}O)$	**145**	116	1.2	**109**	84	1.8	**491**	427	3.4	**502**	437	2.5		
$\tau(C_\alpha{-}C)$	**105**	80	0.1	**79**	57	2.6	**106**	81	1.2	**33**	15	1.3		
$\tau(S{-}C)$	**89**	66	0.9	**43**	24	1.0	**94**	70	0.4	**60**	40	0.1		
$\tau(C{-}S)$	**56**	36	3.1	**110**	85	0.7	**29**	11	1.7	**113**	87	1.9		

[a] Frequencies in cm^{-1}. Intensities in km mol^{-1}. ν, bond stretching, δ, bending, γ, rocking, ω, wagging, tw, twisting, τ, torsion, see Table 2 for definition of symmetry coordinates. Frequencies in italic were those use for force field scaling. [b] Bands marked with * belong to the *s-trans* conformers; the intensity of all the remaining bands are almost exclusively due to the *s-cis* conformers. Except in the cases explicitly indicated in the table, all observed bands are considered to have contributions either from *Cg* and *Ca* conformers or from *Tg* and *Ta* forms. [c] This band has also a small but significant contribution from the corresponding vibration of the *s-trans* forms. [d] $\nu(C_\beta{-}C)$ vibration of *s-trans* conformers also contributes to the total intensity of this band. [e] The $\nu(C_\beta{-}C)$ mode in *s-trans* forms contributes to the total intensity of the band at 934 cm^{-1}. [f] The $\nu(C{-}S)$ mode in *s-trans* forms contributes to the total intensity of the band at 620 cm^{-1}. [g] The $\nu(S{-}C)$ vibration of the *Tg* conformer also contributes to the total intensity of this band. [h] The $\nu(S{-}C)$ vibration of the *Ta* conformer also contributes to the total intensity of this band. [i] The $\nu(S{-}C)$ vibration of *s-trans* conformers also contributes to the total intensity of this band.

this axis. In addition, the considerably lower energy of the *s-cis* forms about the C=C—C=O axis when compared with the *s-trans* forms leads to a prevalence in the observed spectra of features due to *s-cis* conformers. The analysis of the results presented in Tables 6–10 and Fig. 3 and 4 lead to the following conclusions:

(i) Both in hexane and deuteriated acetonitrile (CD_3CN) solution *t*-ETC exists as a mixture of four different conformers, in agreement with the theoretical data for the isolated molecule. In the more polar CD_3CN solvent, those bands ascribable only to the more polar *s-trans* conformers increase in relative intensity [bands at 1675 cm^{-1} and 1163 cm^{-1}, assigned respectively to the $\nu(C{=}O)$ and $\nu(C_\alpha{-}C)$ stretching vibrations of the *s-trans* conformers]. In addition to these bands, several other bands have substantial intensity contributions from the *s-trans* forms, and have also their relative intensities increased in the spectrum of the compound dissolved in the more polar solvent (*e.g.* the bands at *ca.* 1090 and 1060 cm^{-1}). The *s-trans* $\nu(C_\alpha{-}C)$ stretching band at *ca.* 1165 cm^{-1} is of note, as it corresponds to a very intense band appearing in a 'clean' spectral region (see Fig. 3 and 4). Since it is not expected that the $\nu(C_\alpha{-}C)$ stretching mode will change much in frequency in other α,β-unsaturated thioesters (for instance this mode gives rise to a band at *ca.* 1170 cm^{-1} in *S*-ethyl thioacrylate,[20] this band may be used as a probe of the presence of *s-trans* conformers of α,β-unsaturated thioesters in more complex situations (for example, in enzyme active sites).

(ii) The experimental spectra obtained in hexane and CD_3CN solutions are well fitted by the calculations when the calculated spectra of *s-cis* and *s-trans* conformers are added with the *s-trans* spectra multiplied by factors of 1/2.25 and 1/1.70, respectively. As expected, the relative magnitude of these weighting factors agrees with a stabilization of the *s-trans* conformers in the more polar solvent. In addition, assuming a Boltzmann population distribution, the (*s-trans*) – (*s-cis*) energy difference may be estimated to be *ca.* 2.0 and *ca.* 1.5 kJ mol^{-1}, respectively, in hexane and in CD_3CN solu-

Table 7 Normal coordinate analysis for *t*-ETC (form *Cg*)[a]

approximate description	calculated frequency	PED[b]
$\nu(C_\beta-H)$	3371	$S_9(74) + S_8(25)$
$\nu(C_\alpha-H)$	3368	$S_8(75) + S_9(25)$
$\nu(CH_2)_{as}$	3326	$S_{13}(77) + S_{16}(16)$
$\nu(CH_3)_{as}$	3303	$S_{16}(66) + S_{15}(15) + S_{13}(11)$
$\nu(C_\gamma H_3)_{as}$	3288	$S_{10}(97)$
$\nu(CH_3)_{as}$	3271	$S_{13}(73) + S_{16}(18)$
$\nu(CH_2)_s$	3255	$S_{14}(84)$
$\nu(C_\gamma H_3)_{as}$	3253	$S_{11}(101)$
$\nu(CH_3)_s$	3210	$S_{17}(93)$
$\nu(C_\gamma H_3)_s$	3202	$S_{12}(98)$
$\nu(C=O)$	1949	$S_1(92)$
$\nu(C=C)$	1864	$S_4(70) + S_{25}(12)$
$\delta(CH_3)_{as}$	1647	$S_{29}(69) + S_{30}(24)$
$\delta(CH_3)_{as}$	1636	$S_{30}(76) + S_{29}(22)$
$\delta(C_\gamma H_3)_{as}$	1628	$S_{26}(93)$
$\delta(C_\gamma H_3)_{as}$	1623	$S_{27}(94)$
$\delta(CH_2)$	1612	$S_{32}(109)$
$\delta C_\gamma H_3)_s$	1564	$S_{28}(104)$
$\delta(CH_3)_s$	1562	$S_{31}(103)$
$\delta(C_\alpha-H)$	1464	$S_{23}(64) + S_4(10)$
$\omega(CH_2)$	1452	$S_{33}(87)$
$\delta(C_\beta-H)$	1437	$S_{25}(71)$
tw(CH_2)	1408	$S_{34}(64) + S_{39}(17)$
$\gamma(C_\gamma H_3)$	1231	$S_{35}(35) + S_{36}(33)$
$\gamma(C_\gamma H_3)$	1201	$S_{42}(60) + S_{37}(45)$
$\gamma(CH_3)$	1187	$S_{39}(22) + S_3(16) + S_{34}(16) + S_{35}(13)$
$\gamma(CH_3)$	1172	$S_{38}(48) + S_7(21)$
$\nu(C_\alpha-C)$	1152	$S_3(35) + S_{39}(12) + S_{34}(11) + S_{23}(10) + S_2(10)$
$\gamma(C_\alpha-H)$	1102	$S_{41}(40) + S_{37}(19) + S_{42}(16)$
$\nu(C-C)$	1059	$S_7(63) + S_{38}(20)$
$\nu(C_\beta-C)$	996	$S_{36}(38) + S_3(35)$
$\gamma(C_\beta-H)$	915	$S_{42}(40) + S_{37}(19) + S_{40}(16) + S_{41}(16)$
$\nu(C-S)$	901	$S_2(28) + S_{19}(19) + S_{22}(18) + S_{18}(12)$
$\gamma(CH_2)$	829	$S_{35}(71) + S_{39}(43)$
$\nu(S-C)$	728	$S_6(89)$
$\gamma(C=O)$	698	$S_{40}(78) + S_{42}(20) + S_{43}(13) + S_{45}(11)$
$\delta(O=C-S)$	557	$S_2(42) + S_{18}(29) + S_{20}(15)$
$\delta(C-C=C)$	439	$S_{24}(46) + S_{19}(29)$
$\delta(S-C-C)$	392	$S_{21}(45)$
$\delta(C=C-C)$	333	$S_{21}(24) + S_{18}(21) + S_{22}(20)$
$\tau(CH_3)$	295	$S_{48}(56) + S_{20}(22)$
$\tau(C=C)$	226	$S_{43}(64) + S_{42}(12) + S_{48}(10)$
$\delta(C-S-C)$	221	$S_{48}(21) + S_{20}(21) + S_{47}(13) + S_{42}(13)$
$\tau(C_\gamma H_3)$	211	$S_{47}(78)$
$\delta(C-C=O)$	145	$S_{19}(28) + S_{22}(27) + S_{46}(19) + S_{20}(14) + S_{24}(12)$
$\tau(C_\alpha-C)$	105	$S_{44}(60) + S_{45}(27) + S_{46}(21) + S_{47}(11)$
$\tau(S-C)$	89	$S_{46}(56) + S_{45}(12)$
$\tau(C-S)$	56	$S_{45}(47) + S_{46}(31) + S_{41}(19)$

[a] Frequencies in cm^{-1}. ν, bond stretching, δ, bending, γ, rocking, ω, wagging, tw, twisting, τ, torsion, see Table 2 for definition of symmetry coordinates. [b] Only PED values greater than 10% are given.

tion. Although this estimate may have a substantial error, considering that intrinsic band intensities may be significantly different in the isolated molecule situation and for the solutions phases, the magnitude of the differences in energy found is large enough to enable us to conclude that the experimental data point to a considerably smaller energy difference between the two stable conformations about the C=C—C=O axis for *t*-ETC in solution than for the isolated molecule (*ca.* 7 kJ mol^{-1}).

(iii) Similarly to the case of *c*-ETC, it is not possible to identify, in the IR spectra of *t*-ETC, many bands ascribable to a single conformer differing in the relative position of the C—S—C—C axis. In fact, with the exception of the $\delta(CH_2)$ bending vibration of the *Cg* form, ascribed to the band at 1416 cm^{-1}, all modes which are predicted to have significantly different frequencies in the *gauche* and *anti* C—S—C—C forms have frequencies nearly coincident with those of different modes, and have been ascribed to bands which also have contributions from these latter vibrations [for example, the $\delta(CH_3)$ symmetric bending modes of *Cg* and *Ca* contribute to the total intensities of the bands at 1375 and 1300 cm^{-1}, also assigned to the $\delta(C_\gamma H_3)$ symmetric and $\delta(C_\alpha-H)$ bending vibrations, respectively (see Table 6)]. The bands observed at 635 cm^{-1} and 661 cm^{-1} [$\nu(S-C)$] are a slight exception to the above rule: each one contains significant contributions from the two conformers having the same conformation of the C—S—C—S axis but different conformation around the C=C—C=O axis. In fact, the calculations clearly indicate that the intensity of the $\nu(S-C)$ vibration is much higher in the *s-trans* than in the corresponding *s-cis* conformers, while the frequencies depend only on the relative orientation of the C—S—C—C axis, being larger for the *anti* conformation. Thus, the 635 cm^{-1} band is here assigned to $\nu(S-C)$ in both *Cg* and *Tg* conformers, while the 661 cm^{-1} band is ascribed to the same mode in the two symmetric forms (*Ca* and *Ta*).

(iv) Also as was found for *c*-ETC, the experimental frequencies for $\nu(C=C)$ and $\nu(C=O)$ in *t*-ETC are significantly

Table 8 Normal coordinate analysis for *t*-ETC (form *Ca*)[a]

approximated description		calculated frequency	PED[b]
$\nu(\mathrm{C_\beta{-}H})$	A′	3370	$S_9(85) + S_8(14)$
$\nu(\mathrm{C_\alpha{-}H})$	A′	3367	$S_8(86) + S_9(14)$
$\nu(\mathrm{CH_2})_{\mathrm{as}}$	A″	3328	$S_{13}(95)$
$\nu\mathrm{C_\gamma H_3)_{as}}$	A′	3288	$S_{10}(97)$
$\nu(\mathrm{CH_3})_{\mathrm{as}}$	A′	3282	$S_{15}(67) + S_{14}(34)$
$\nu(\mathrm{CH_3})_{\mathrm{as}}$	A″	3279	$S_{16}(96)$
$\nu(\mathrm{CH_2})_{\mathrm{s}}$	A′	3268	$S_{14}(67) + S_{15}(34)$
$\nu(\mathrm{C_\gamma H_3})_{\mathrm{as}}$	A″	3253	$S_{11}(101)$
$\nu(\mathrm{CH_3})_{\mathrm{s}}$	A′	3212	$S_{17}(100)$
$\nu(\mathrm{C_\gamma H_3})_{\mathrm{s}}$	A′	3200	$S_{12}(88)$
$\nu(\mathrm{C{=}O})$	A′	1951	$S_1(92)$
$\nu(\mathrm{C{=}C})$	A′	1865	$S_4(70) + S_{25}(12)$
$\delta(\mathrm{CH_3})_{\mathrm{as}}$	A′	1646	$S_{29}(86)$
$\delta(\mathrm{CH_3})_{\mathrm{as}}$	A″	1640	$S_{30}(100)$
$\delta(\mathrm{CH_2})$	A′	1629	$S_{32}(93)$
$\delta(\mathrm{C_\gamma H_3})_{\mathrm{as}}$	A′	1628	$S_{26}(88)$
$\delta(\mathrm{C_\gamma H_3})_{\mathrm{as}}$	A″	1623	$S_{27}(94)$
$\delta(\mathrm{CH_3})_{\mathrm{s}}$	A′	1567	$S_{31}(104)$
$\delta(\mathrm{C_\gamma H_3})_{\mathrm{s}}$	A′	1464	$S_{28}(104)$
$\delta(\mathrm{C_\alpha{-}H})$	A′	1465	$S_{23}(61)$
$\omega(\mathrm{CH_2})$	A′	1445	$S_{33}(80)$
$\delta(\mathrm{C_\beta{-}H})$	A′	1437	$S_{25}(68)$
$\mathrm{tw}(\mathrm{CH_2})$	A″	1384	$S_{34}(56) + S_{39}(22)$
$\gamma(\mathrm{C_\gamma H_3})$	A′	1231	$S_5(35) + S_{36}(33)$
$\gamma(\mathrm{C_\gamma H_3})$	A″	1201	$S_{42}(60) + S_{37}(45)$
$\gamma(\mathrm{CH_3})$	A′	1182	$S_{38}(38) + S_3(10) + S_7(15)$
$\gamma(\mathrm{CH_3})$	A″	1164	$S_{34}(39) + S_{39}(32) + S_{35}(28)$
$\nu(\mathrm{C_\alpha{-}C})$	A′	1155	$S_3(36) + S_{38}(19) + S_{23}(10)$
$\gamma(\mathrm{C_\alpha{-}H})$	A″	1102	$S_{41}(39) + S_{37}(19) + S_{42}(16)$
$\nu(\mathrm{C{-}C})$	A′	1064	$S_7(67) + S_{38}(15)$
$\nu(\mathrm{C_\beta{-}C})$	A′	996	$S_{36}(38) + S_5(36)$
$\gamma(\mathrm{C_\beta{-}H})$	A″	916	$S_{42}(40) + S_{37}(19) + S_{40}(16) + S_{41}(16)$
$\nu(\mathrm{C{-}S})$	A′	903	$S_2(28) + S_{19}(19) + S_{22}(18) + S_{18}(12)$
$\gamma(\mathrm{CH_2})$	A″	850	$S_{35}(71) + S_{39}(43)$
$\nu(\mathrm{S{-}C})$	A′	755	$S_6(85) + S_{38}(10)$
$\gamma(\mathrm{C{=}O})$	A″	697	$S_{40}(78) + S_{42}(20) + S_{43}(14) + S_{45}(11)$
$\delta(\mathrm{O{=}C{-}S})$	A′	575	$S_2(42) + S_{18}(22) + S_{20}(11)$
$\delta(\mathrm{C{-}C{=}C})$	A′	436	$S_{24}(54) + S_{19}(30)$
$\delta(\mathrm{C{=}C{-}C})$	A′	378	$S_{18}(35) + S_{21}(30) + S_{22}(14)$
$\delta(\mathrm{S{-}C{-}C})$	A′	313	$S_{21}(30) + S_2(16)$
$\tau(\mathrm{CH_3})$	A″	265	$S_{48}(98)$
$\tau(\mathrm{C{=}C})$	A″	225	$S_{43}(69) + S_{42}(13) + S_{41}(10)$
$\delta(\mathrm{C{-}S{-}C})$	A′	219	$S_{20}(40) + S_{22}(27) + S_{24}(20) + S_{21}(15) + S_{18}(13)$
$\tau(\mathrm{C_\gamma H_3})$	A″	212	$S_{47}(86)$
$\tau(\mathrm{C{-}S})$	A″	110	$S_{45}(50) + S_{44}(47) + S_{47}(11)$
$\delta(\mathrm{C{-}C{=}O})$	A′	109	$S_{20}(31) + S_{19}(28) + S_{22}(19) + S_{18}(13) + S_{21}(11)$
$\tau(\mathrm{C_\alpha{-}C})$	A″	79	$S_{44}(37) + S_{46}(36) + S_{43}(26) + S_{45}(16) + S_{41}(16)$
$\tau(\mathrm{S{-}C})$	A″	43	$S_{46}(73) + S_{45}(14) + S_{44}(13) + S_{43}(13)$

[a] Frequencies in cm^{-1}. ν, bond stretching; δ, bending, γ, rocking, ω, wagging, tw, twisting, τ, torsion, see Table 2 for definition of symmetry coordinates.[b] Only PED values greater than 10% are given.

smaller than the calculated (scaled) values, pointing to an increased polarity of these bonds (less double-bond character) due to intermolecular interactions with the solvent. As expected, the frequency red shift is considerably more pronounced when the solvent is CD$_3$CN. In addition, the red shifts are also more relevant for $\nu(\mathrm{C{=}O})$ than for $\nu(\mathrm{C{=}C})$ and, for the same mode and solvent, for the more polar *s*-trans conformers (Table 6).

(v) Finally, also for this molecule $\nu(\mathrm{S{-}C})$ is an essentially pure mode whichever conformer is considered [Table 7–10, in *Tg* this coordinate mixes somewhat with the $\nu(\mathrm{C{-}S})$ coordinate], while both $\nu(\mathrm{C_\alpha{-}C})$ and $\nu(\mathrm{C{-}S})$ are considerably mixed modes. Particularly relevant is the fact that $\nu(\mathrm{C{-}S})$ reduces its frequency by *ca.* 190 cm^{-1} in going from the *s-cis* to the *s-trans* C═C—C═O axis conformation. Indeed, in both *Cg* and *Ca* forms, this mode gives rise to a band nearly at the same position as in *c*-ETC (810 *vs.* 820 cm^{-1}), while $\nu(\mathrm{C{-}S})$ in the *Tg* and *Ta* conformers contributes to the total intensity of the band at *ca.* 620 cm^{-1}, also ascribed to the $\gamma(\mathrm{C{=}O})$ out-of-plane bending vibration. An interesting conclusion that can be derived from these data and that may be important to the analysis of the α,β-unsaturated thiolacylenzyme vibrational data is that assuming the *s-trans* conformation about the C$_\alpha$—C axis leads to a weakening of the catalytically relevant C—S bond. The importance of this result is underlined by the fact that the structural data do not reflect such a weakening (the C—S bond lengths are nearly equal in the *s-cis* and *s-trans* forms, Table 1), because the changes with conformation of the relevant intramolecular interactions, which determine the bond lengths in the two forms, compensate each other.

R.F. acknowledges financial support from Junta Nacional de Investigacão Cientifica e Tecnológica, J.N.C.I.T., Lisboa.

Table 9 Normal coordinate analysis for *t*-ETC (form *Tg*)[a]

approximate description	calculated frequency	PED[b]
$\nu(C_\alpha-H)$	3370	$S_8(98)$
$\nu(C_\beta-H)$	3358	$S_9(97)$
$\nu(CH_2)_{as}$	3329	$S_{13}(78) + S_{16}(12)$
$\nu(CH_3)_{as}$	3304	$S_{16}(69) + S_{15}(15)$
$\nu(C_\gamma H_3)_{as}$	3290	$S_{10}(96)$
$\nu(CH_3)_{as}$	3271	$S_{15}(74) + S_{16}(18)$
$\nu(CH_2)_s$	3255	$S_{14}(83) + S_{13}(11)$
$\nu(C_\gamma H_3)_{as}$	3254	$S_{11}(101)$
$\nu(CH_3)_s$	3210	$S_{17}(92)$
$\nu(C_\gamma H_3)_s$	3202	$S_{12}(97)$
$\nu(C{=}O)$	1951	$S_1(93)$
$\nu(C{=}C)$	1877	$S_4(70) + S_{25}(13)$
$\delta(CH_3)_{as}$	1647	$S_{29}(69) + S_{30}(24)$
$\delta(CH_3)_{as}$	1636	$S_{30}(76) + S_{29}(22)$
$\delta(C_\gamma H_3)_{as}$	1629	$S_{26}(94)$
$\delta C_\gamma H_3)_{as}$	1622	$S_{27}(95)$
$\delta(CH_2)$	1612	$S_{32}(110)$
$\delta(C_\gamma H_3)_s$	1565	$S_{28}(104)$
$\delta(CH_3)_s$	1562	$S_{31}(103)$
$\delta(C_\beta-H)$	1460	$S_{25}(68) + S_4(13)$
$\omega(CH_2)$	1452	$S_{33}(89)$
$\delta(C_\alpha-H)$	1423	$S_{23}(70)$
tw(CH_2)	1408	$S_{34}(62) + S_{39}(17)$
$\nu(C_\alpha-C)$	1298	$S_3(41) + S_2(12) + S_{18}(12) + S_{22}(10)$
$\gamma(C_\gamma H_3)$	1194	$S_{37}(52) + S_{42}(35) + S_5(10)$
$\gamma(C_\gamma H_3)$	1193	$S_5(22) + S_{37}(15) + S_{42}(14) + S_{36}(12)$
$\gamma(CH_3)$	1172	$S_{38}(53) + S_7(25)$
$\gamma(CH_3)$	1169	$S_{39}(31) + S_{34}(25) + S_{35}(16) + S_5(10)$
$\gamma(C_\alpha-H)$	1107	$S_{41}(49) + S_{42}(16) + S_{37}(12)$
$\nu(C-C)$	1059	$S_7(63) + S_{38}(21)$
$\nu(C_\beta-C)$	1024	$S_{36}(44) + S_5(33) + S_{25}(10)$
$\gamma(C_\beta-H)$	923	$S_{42}(46) + S_{37}(18) + S_{40}(17) + S_{41}(12)$
$\gamma(CH_2)$	831	$S_{35}(65) + S_{39}(39)$
$\nu(S-C)$	739	$S_6(65) + S_2(15) + S_{18}(10)$
$\nu(C-S)$	696	$S_2(31) + S_6(23) + S_{19}(13) + S_{24}(13)$
$\gamma(C{=}O)$	673	$S_{40}(73) + S_{42}(23) + S_{43}(14)$
$\delta(O{=}C-S)$	609	$S_{18}(27) + S_{22}(20) + S_{20}(12) + S_{19}(10)$
$\delta(C-C{=}O)$	491	$S_2(31) + S_{19}(20) + S_{18}(14)$
$\delta(S-C-C)$	387	$S_{21}(52) + S_{24}(16)$
$\delta(C-C{=}C)$	330	$S_{24}(38) + S_{21}(22) + S_{18}(19)$
$\tau(CH_3)$	297	$S_{48}(57) + S_{20}(24)$
$\tau(C_\gamma H_3)$	220	$S_{47}(30) + S_{43}(26) + S_{48}(20) + S_{41}(17) + S_{20}(15)$
$\delta(C-S-C)$	214	$S_{20}(25) + S_{47}(33) + S_{48}(23) + S_{43}(10)$
$\tau(C{=}C)$	197	$S_{43}(58) + S_{47}(15) + S_{42}(10)$
$\delta(C{=}C-C)$	150	$S_{22}(29) + S_{19}(28) + S_{46}(11) + S_{24}(10)$
$\tau(C_\alpha-C)$	106	$S_{44}(66) + S_{46}(27)$
$\tau(S-C)$	94	$S_{46}(66) + S_{44}(11) + S_{45}(11)$
$\tau(C-S)$	29	$S_{45}(74) + S_{44}(15)$

[a] Frequencies in cm^{-1}. ν, bond stretching, δ, bending, γ rocking, ω, wagging, tw, twisting, τ, torsion, see Table 2 for definition of symmetry coordinates. [b] Only PED values greater than 10% are given.

Table 10 Normal coordinate analysis for *t*-ETC (form *Ta*)[a]

approximate description		calculated frequency	PED[b]
$\nu(C_\alpha{-}H)$	A′	3369	$S_8(99)$
$\nu(C_\beta{-}H)$	A′	3356	$S_9(97)$
$\nu(CH_2)_{as}$	A″	3332	$S_{13}(96)$
$\nu(C_\gamma H_3)_{as}$	A′	3290	$S_{10}(96)$
$\nu(CH_3)_{as}$	A′	3283	$S_{15}(57) + S_{14}(43)$
$\nu(CH_3)_{as}$	A″	3279	$S_{16}(97)$
$\nu(CH_2)_s$	A′	3270	$S_{14}(57) + S_{15}(44)$
$\nu(C_\gamma H_3)_{as}$	A″	3254	$S_{11}(101)$
$\nu(CH_3)_s$	A′	3212	$S_{17}(100)$
$\nu(C_\gamma H_3)_s$	A′	3202	$S_{12}(97)$
$\nu(C{=}O)$	A′	1953	$S_1(94)$
$\nu(C{=}C)$	A′	1878	$S_4(70) + S_{25}(13)$
$\delta(CH_3)_{as}$	A′	1646	$S_{29}(86)$
$\delta(CH_3)_{as}$	*A″*	1640	$S_{30}(100)$
$\delta(CH_2)$	A′	1629	$S_{32}(95)$
$\delta(C_\gamma H_3)_{as}$	A′	1629	$S_{26}(92)$
$\delta(C_\gamma H_3)_{as}$	A″	1622	$S_{27}(95)$
$\delta(CH_3)_s$	A′	1567	$S_{31}(104)$
$\delta(C_\gamma H_3)_s$	A′	1465	$S_{28}(104)$
$\delta(C_\beta{-}H)$	A′	1461	$S_{25}(68) + S_4(13)$
$\omega(CH_2)$	A′	1446	$S_{33}(87)$
$\delta(C_\alpha{-}H)$	A′	1422	$S_{23}(72)$
tw(CH_2)	A″	1384	$S_{34}(56) + S_{39}(22)$
$\nu(C_\alpha{-}C)$	A′	1299	$S_3(41) + S_2(12) + S_{18}(12) + S_{23}(10)$
$\gamma(C_\gamma H_3)$	A″	1193	$S_{37}(52) + S_{42}(49)$
$\gamma(C_\gamma H_3)$	A′	1191	$S_5(36) + S_{36}(19) + S_3(16)$
$\gamma(CH_3)$	A′	1170	$S_{38}(48) + S_7(18)$
$\gamma(CH_3)$	A″	1164	$S_{34}(39) + S_{39}(32) + S_{35}(28)$
$\gamma(C_\alpha{-}H)$	A″	1107	$S_{41}(49) + S_{42}(16) + S_{37}(12)$
$\nu(C{-}C)$	A′	1064	$S_7(67) + S_{38}(15)$
$\nu(C_\beta{-}C)$	A′	1024	$S_{36}(44) + S_5(33) + S_{25}(10)$
$\gamma(C_\beta{-}H)$	A″	923	$S_{42}(46) + S_{37}(18) + S_{40}(17)$
$\gamma(CH_2)$	A″	851	$S_{35}(72) + S_{39}(43)$
$\nu(S{-}C)$	A′	763	$S_6(77)$
$\nu(C{-}S)$	A′	708	$S_2(50) + S_{24}(15) + S_{19}(14) + S_3(10)$
$\gamma(C{=}O)$	A″	674	$S_{40}(74) + S_{42}(25) + S_{43}(15)$
$\delta(O{=}C{-}S)$	A′	610	$S_{18}(29) + S_{22}(20) + S_6(10)$
$\delta(C{-}C{=}O)$	A′	502	$S_{19}(27) + S_2(23) + S_{22}(10)$
$\delta(S{-}C{-}C)$	A′	363	$S_{21}(33) + S_{18}(27) + S_{24}(26)$
$\delta(C{-}C{=}C)$	A′	326	$S_{21}(26) + S_{24}(24) + S_2(11)$
$\tau(CH_3)$	A″	265	$S_{18}(100)$
$\tau(C_\gamma H_3)$	A″	218	$S_{47}(59) + S_{43}(40) + S_{41}(28)$
$\delta(C{=}C{-}C)$	A′	210	$S_{20}(47) + S_{22}(32) + S_{21}(12)$
$\tau(C{=}C)$	A″	197	$S_{43}(58) + S_{47}(15) + S_{41}(10) + S_{42}(10)$
$\delta(C{-}S{-}C)$	A′	115	$S_{20}(32) + S_{19}(26) + S_{22}(16) + S_{21}(13)$
$\tau(C{-}S)$	A″	113	$S_{45}(94) + S_{44}(18)$
$\tau(S{-}C)$	A″	60	$S_{46}(94) + S_{44}(18)$
$\tau(C_\alpha{-}C)$	A″	33	$S_{44}(37) + S_{46}(36) + S_{45}(16)$

[a] Frequencies in cm^{-1}. ν, bond stretching, δ, bending, γ, rocking, tw, twisting, τ, torsion, see Table 2 for definition of symmetry coordinates.

[b] Only PED values greater than 10% are given.

References

1 P. R. Carey and P. J. Tonge, *Chem. Soc. Rev.*, 1990, **19**, 293.
2 P. J. Tonge and P. R. Carey, *Biochemistry*, 1992, **31**, 9122.
3 P. J. Tonge and P. R. Carey, *J. Mol. Liq.*, 1989, **42**, 195.
4 M. Kim, H. Owen and P. R. Carey, *Appl. Spectrosc.*, 1993, **47**, 1780.
5 V. E. Anderson, P. R. Carey and P. J. Tonge, unpublished work.
6 W. J. Hehre, R. Ditchfield and J. A. Pople, *J. Chem. Phys.*, 1972, **56**, 2257.
7 M. J. Frisch, G. W. Trucks, M. Head-Gordon, P. M. W. Gill, M. W. Wong, J. B. Foresman, B. J. Johnson, H. B. Schlegel, M. A. Robb, E. S. Replogle, R. Gomperts, J. L. Andres, K. Raghavachari, J. S. Binkley, C. Gonzalez, R. L. Martin, D. J. Fox, D. J. Defrees, J. Baker, J. J. P. Stewart and J. A. Pople, GAUSSIAN 92 (*Revision C*). Gaussian Inc., Pittsburgh PA, 1992.
8 H. B. Schlegel, Ph.D. Thesis, Queen's University, Kingston, Ontario, 1975.
9 M. D. G. Faria and R. Fausto, TRANSFORMER (*version 1.0*), Departamento de Química, Universidade de Coimbra, Portugal, 1990).
10 M. D. G. Faria and R. Fausto, BUILD-G and VIBRAT, Departamento de Química, Universidade de Coimbra, Portugal, 1990 (These programs incorporate several routines from programs GMAT and FPERT, H. Fuher, V. B. Kartha, K. G. Kidd, P. J. Krueger and H. H. Mantsch, *Natl. Res. Council Can. Bull.*, 1976, **15**, 1).
11 R. Fausto and J. J. C. Teixeira-Dias, *J. Mol. Struct.* (*Theochem.*), 1987, **150**, 381.
12 R. Fausto, L. A. E. Batista de Carvalho, J. J. C. Teixeira-Dias and M. N. Ramos, *J. Chem. Soc., Faraday Trans. 2*, 1989, **85**, 1945.
13 R. Fausto, L. A. E. Batista de Carvalho and J. J. C. Teixeira-Dias, *J. Mol. Struct.* (*Theochem.*), 1990, **207**, 67.
14 R. Fausto, *J. Mol. Struct.* (*Theochem.*), in the press.
15 R. Fausto, A. G. Martins, J. J. C. Teixeira-Dias, P. J. Tonge and P. R. Carey, *J. Mol. Struct.*, 1994, **59**, 323.
16 R. Fausto, A. G. Martins, J. J. C. Teixeira-Dias, P. J. Tonge and P. R. Carey, *J. Phys. Chem.*, 1994, **98**, 3592.
17 M. D. G. Faria, J. J. C. Teixeira-Dias and R. Fausto, *Vibrat. Spectrosc.*, 1991, **1**, 43.
18 M. D. G. Faria, J. J. C. Teixeira-Dias and R. Fausto, *Vibrat. Spectrosc.*, 1991, **2**, 107.
19 M. D. G. Faria, J. J. C. Teixeira-Dias and R. Fausto, *J. Raman Spectrosc.*, 1991, **22**, 519.
20 P. J. Tonge, P. R. Carey and R. Fausto, to be published.

Paper 4/04662E; *Received* 29*th July*, 1994